Measurement of the Zeeman-like ac Stark shift

Chang Yong Park, Heeso Noh, Chung Mok Lee, and D. Cho*
Department of Physics, Korea University, Seoul 136-701, Korea
(Received 4 May 2000; revised manuscript received 25 August 2000; published 9 February 2001)

We demonstrate that when laser light is circularly polarized and properly detuned, the ac Stark shift of an alkali-metal atom in its ground state takes the form of a pure Zeeman shift. The condition is satisfied when the laser frequency is between the $D1$ and $D2$ transition frequencies, with the size of the detuning from the $D2$ resonance twice that from the $D1$ resonance. The direction of the effective magnetic field is along the laser propagation axis, and its magnitude is proportional to the vector polarizability of the atom and to the laser intensity. We use stimulated Raman spectroscopy on an optically pumped slow atomic beam from a magneto-optical trap to measure the vector polarizability and saturated absorption spectroscopy to show that the scalar polarizability vanishes at the particular detuning.

DOI: 10.1103/PhysRevA.63.032512 PACS number(s): 32.10.Dk, 32.60.+i

I. INTRODUCTION

The ac Stark effect is the result of an interaction between an oscillating electric field and an atom. The electric field induces an electric dipole moment in the atom, and the induced moment interacts with the field again to produce an energy shift, the ac Stark shift. The shift can be a problem in a precision measurement [1], but a field gradient leads to an optical dipole force, which is useful in the study of cooling and trapping of atoms [2] and in atom optics [3].

The ac Stark shift of an atom in its ground state consists of two components due to the scalar and vector polarizabilities. The scalar part is from the induced electric dipole moment parallel to the electric field, and the vector part is from the moment perpendicular to the field. It has been known since 1972 [4] that when the light is circularly polarized, the vector part results in an energy shift analogous to a Zeeman shift. This ''fictitious magnetic field'' was used to demonstrate optically induced spin echoes [5] and spin precessions [6]. In most studies of this phenomenon, the atom is modeled as a two-level system with Zeeman substructure and a near resonant light beam is used to make the effect large. When the ac Stark shift is used to produce a dipole force, however, it is often advantageous to have a far detuned light beam to reduce unwanted photon scattering. In this case the multilevel nature of an atom becomes important. For alkali atoms, which play a central role in both precision measurements and atom optics, the fine structure, whose spin-orbit coupling is responsible for the vector polarizability, is important. We pointed out [7] that when the laser light is properly detuned between the $D1$ and $D2$ transitions of an alkali-metal atom, the scalar polarizability vanishes and the contributions from the $D1$ and $D2$ couplings to the vector polarizability add constructively. When this condition is satisfied and the laser light is circularly polarized, the ac Stark shift takes the same form as a Zeeman shift, and the laser intensity gradient produces a pure Stern-Gerlach type force.

Using the Zeeman-like ac Stark effect one may replace a magnetic field with a laser beam when such a replacement leads to a more convenient or interesting experimental situation. The laser-induced Stern-Gerlach force provides a new tool in optically manipulating atomic motion in a spin-dependent way. Recently it was used in an experiment where an optical dipole trap, which behaved like a magnetic trap, was constructed to trap spin-polarized rubidium atoms [8]. In the spin precession experiment [6] a similar situation was exploited for lithium atoms. It is also possible to perform the classic Stern-Gerlach experiment using a laser intensity gradient in place of a magnetic-field gradient, or to produce a standing wave along which the effective magnetic-field strength changes from zero to maximum in half a wavelength of the light. Such a ''magnetic grating'' cannot be built with conventional coils.

In this paper we briefly outline the theory and report the spectroscopic measurement of the Zeeman-like ac Stark shift. In the first part of the experiment we study the vector part under various detunings and polarizations of the laser light using a slow atomic beam from a magneto-optical trap. We apply the standard atomic beam resonance methods including optical pumping, stimulated Raman excitation, and detection by shelving technique to the slow atomic beam. The experimental procedures are described in detail. In the second part we show that the scalar polarizability vanishes at the expected detuning using saturated absorption spectroscopy in a vapor cell.

II. THEORY

When an alkali-metal atom in its ground state $|nS_{1/2},m_j\rangle$ is irradiated by a laser field $\mathbf{E}(t)=\mathcal{E}_0 e^{-i\omega t}+\mathcal{E}_0^* e^{i\omega t}$, its ac Stark shift, to the lowest order, is

$$U(nS_{1/2},m_j)=\alpha(\omega)\mathcal{E}_0\cdot\mathcal{E}_0^* + i\beta(\omega)(\mathcal{E}_0^*\mathcal{E}_0)\cdot\langle S_{1/2},m_j|\boldsymbol{\sigma}|S_{1/2},m_j\rangle. \quad (1)$$

Here α and β are the scalar and vector polarizabilities, respectively, and $\boldsymbol{\sigma}$ is the Pauli spin operator [9]. Explicit forms of the polarizabilities are given in Ref. [7]. The vector part vanishes either in the dc Stark effect or when the applied light is linearly polarized. However, when the light is circu-

*Email address: cho@korea.ac.kr

larly polarized, $\mathcal{E}_0=\varepsilon_0(\hat{x}+i\hat{y})/\sqrt{2}$, the vector part produces a shift analogous to a Zeeman shift:

$$U(nS_{1/2},m_j)=\alpha(\omega)|\varepsilon_0|^2-\beta(\omega)|\varepsilon_0|^2 g_j m_j, \qquad (2)$$

where g_j is the Lande g factor.

When the laser is tuned near the alkali-metal D transitions, the scalar and vector polarizabilities take the approximate forms

$$\alpha(\omega)\simeq\frac{|\langle nS_{1/2}|er|nP_{1/2}\rangle|^2}{9}\left[\frac{1}{\Delta_{1/2}}+\frac{2}{\Delta_{3/2}}\right], \qquad (3)$$

$$\beta(\omega)\simeq\frac{|\langle nS_{1/2}|er|nP_{1/2}\rangle|^2}{9}\left[\frac{1}{\Delta_{1/2}}-\frac{1}{\Delta_{3/2}}\right], \qquad (4)$$

where $\Delta_{1/2}=\hbar\omega-(E_{nP_{1/2}}-E_{nS_{1/2}})$ and $\Delta_{3/2}=\hbar\omega-(E_{nP_{3/2}}-E_{nS_{1/2}})$. For the above expressions we consider only $nS-nP$ coupling and neglect the farther off-resonance terms. We also assume the same dipole matrix element for the $D1$ and $D2$ couplings. It is obvious from Eq. (4) that the vector polarizability would have vanished if the $nP_{1/2}$ and $nP_{3/2}$ states were degenerate. In most of the experimental situations, where the dipole force is used, the laser light is either blue or red detuned with respect to both $D1$ and $D2$ transitions. For example, in a typical far-off-resonance optical trap [10] the laser is far red detuned with respect to the $D1$ transition. The situation is shown in Fig. 1(a). Because α is the sum of the $D1$ and $D2$ couplings and β is the difference, β is generally a small fraction of α. When the laser is detuned between the $D1$ and $D2$ transitions, however, the situation is reversed. In fact, when $\Delta_{3/2}=-2\Delta_{1/2}$, as in Fig. 1(b), the scalar polarizability identically vanishes and only the vector polarizability term remains. Under this condition, the ac Stark shift takes the form of a pure Zeeman shift, $U(nS_{1/2},m_j)=-\beta(\omega)|\varepsilon_0|^2 g_j m_j$. The effective magnetic field is along the direction of the laser propagation and its magnitude is $\beta|\varepsilon_0|^2/\mu_B$ where μ_B is the Bohr magneton. The effective field can be either parallel or antiparallel to the laser propagation depending on the light helicity. When 1 W of laser power is focused to a spot size ($1/e^2$ radius of an intensity profile) of 10 μm, the effective magnetic field at the focus is 250 G for rubidium. For lighter atoms like sodium, whose fine structure splitting is only one tenth of that for rubidium, the effective field can be as large as 2500 G, but the photon scattering rate is 100 times higher.

III. MEASUREMENT OF THE ac STARK SHIFT

We use rubidium atoms in our study of the Zeeman-like ac Stark shift. In the theory of Sec. II we neglected the hyperfine structure. Because the relevant detuning is three orders of magnitude larger than the ground-state hyperfine structure for a heavy alkali atom like rubidium, Eq. (2) remains a good approximation with the simple replacement of $g_j m_j$ with $g_F m_F$. Here F is the total angular momentum. Because the scalar part is the same for all states in the ground level, we use the hyperfine transition to study the vector part independently in order to show that the shift takes the form of a Zeeman shift. For the scalar part we use the cycling transition of the $D2$ lines to show that the scalar polarizability vanishes at $\lambda\cong 790$ nm.

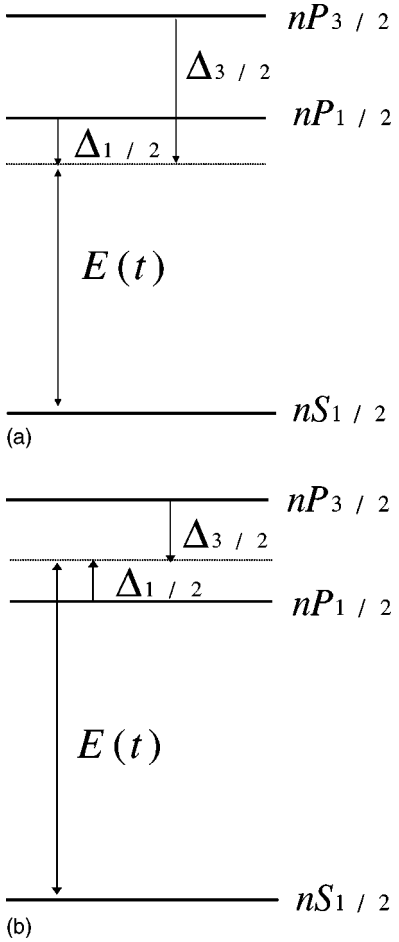

FIG. 1. (a) The laser is red detuned with respect to both $D1$ and $D2$ transitions. Δ's are the detunings defined in the text. (b) The laser is detuned between the $D1$ and $D2$ transitions so that $\Delta_{3/2}=-2\Delta_{1/2}$.

A. Vector polarizability

The frequency shift of the transition from $|nS,F,m_F\rangle$ to $|nS,F+1,m_F\rangle$ due to circularly polarized laser light is $\delta f=2\beta(\omega)|\varepsilon_0|^2|g_F|m_F$. We use ^{87}Rb, whose g_F for $F=1$ and $F=2$ are $-1/2$ and $1/2$, respectively. The measurement is basically the same as a standard magnetic-resonance experiment using a spin-polarized atomic beam [11]. However, unlike the static magnetic field, which can be applied over a large area, the interaction region is limited to a tightly focused laser beam (Stark beam). This localization leads to two difficulties in the measurement. The first one is the transit-time limited linewidth. If the Stark beam has a spot size ω_0, then the frequency shift scales with $1/\omega_0^2$ and the linewidth with $1/\omega_0$. In principle we can make the frequency shift larger than the linewidth by reducing ω_0. The number of atoms interacting with the Stark beam, however, is proportional to ω_0, and the resulting signal size for thermal beams is impractically small. For example, when the Stark beam

power is 1 W and the atomic velocity is 300 m/s, the shift and the width become comparable when the spot size is on the order of 100 μm. In order to increase the transit time we use the slow atomic beam produced from magneto-optically trapped atoms. This type of beam source was developed by Lu *et al.* [12], and it is called a low-velocity intense source (LVIS). It can produce up to 5×10^9 atoms/s at a beam velocity less than 15 m/s. The second difficulty is that we must localize the microwave power so that only those atoms inside the focused Stark beam may undergo the 6.8 GHz transition from the $F=1$ to the $F=2$ hyperfine level of ^{87}Rb. This rules out a direct application of the microwave radiation, so we use stimulated Raman spectroscopy. We modulate the injection current to a laser diode at 3.4 GHz and the resulting pair of first-order sidebands have the correct frequency difference to coherently drive the hyperfine transition. We can localize the transition region by simply focusing the Raman laser beam.

The apparatus consists of four parts. The first part is the LVIS constructed from a magneto-optical trap. Our LVIS setup uses standard ultrahigh vacuum components with rubidium getters and external-cavity diode lasers (described in Ref. [13]). We operate the LVIS in a pulsed mode and it takes more than 15 ms for the pulse of atoms to reach the interaction region. We can turn off the laser and magnetic field required for the LVIS in only a few msec so that they do not interfere with the measurement at the interaction region. The pulse of atoms are optically pumped into $|5S_{1/2},F=1,m_F=1\rangle$ by a linearly polarized laser beam tuned to $|5S_{1/2},F=2\rangle-|5P_{3/2},F'=2\rangle$ for the ''hyperfine pumping'' and by a circularly polarized laser beam tuned to $|5S_{1/2},F=1\rangle-|5P_{3/2},F'=1\rangle$ for the ''Zeeman pumping.'' The laser beams are supplied by two frequency-stabilized external cavity diode lasers. The quantization axis, the z axis, is transverse to the atomic beam direction and defined by a 2.55-G magnetic field produced by a Helmholtz coil. The magnetic field is uniform across both the optical pumping region and the interaction region.

In the third part, the spin-polarized atoms interact with the Stark beam from a Ti:Sapphire laser focused to a spot size of 0.98 mm. Overlapped with the Stark beam is the circularly polarized Raman beam with a somewhat smaller spot size. The Stark beam and Raman beam are counterpropagating along the *z* axis. The Ti:Sapphire laser frequency is free running but its power is kept constant by a servo system with a fast photodiode and an acousto-optical modulator. The carrier of the Raman laser is locked to the saturated absorption signal from the $|5S_{1/2},F=3\rangle-|5P_{3/2},F'=3\rangle$ transition of ^{85}Rb, which is blue detuned by 1.5 GHz from the $|5S_{1/2},F=2\rangle-|5P_{3/2},F'=1\rangle$ transition of ^{87}Rb due to the isotope shift. Then the lower and upper sidebands are red detuned by 1.9 GHz from the $|5S_{1/2},F=2\rangle-|5P_{3/2},F'=1\rangle$ and $|5S_{1/2},F=1\rangle-|5P_{3/2},F'=0\rangle$ transitions, respectively. The Raman laser is also the external-cavity type with a grating. Its cavity length is adjusted so that its free spectral range is 3.4 GHz. This adjustment and the relaxation oscillation of the laser diode near 3 GHz allows us to put more than 20% of the output power into the first-order sidebands. We use a yttrium iron garnet (YIG) tuned oscillator with 25 mW output power as a microwave source without further amplification.

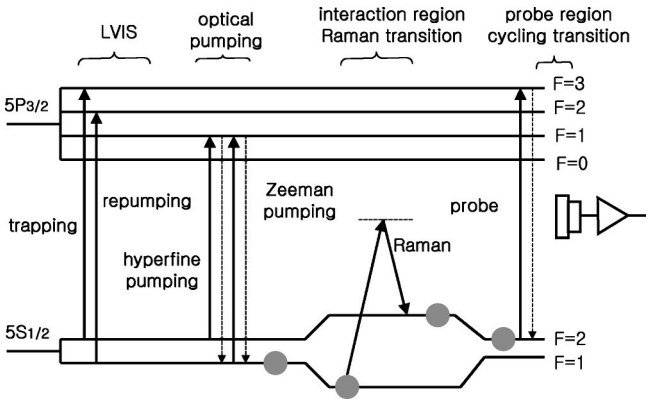

FIG. 2. The beam resonance method with the shelving technique used in the measurement of the vector polarizability.

Finally, the Raman transition is detected in the probe region, where we shine a laser tuned to the cycling transition of $|5S_{1/2},F=2\rangle$ to $|5P_{3/2},F'=3\rangle$. Those atoms that have made a Raman transition to $|5S_{1/2},F=2,m_F\rangle$ scatter many photons which are detected by a large area photodiode. The background from the atoms that survive the hyperfine pumping and remain in the $F=2$ state is negligible. However, scattering of the strong Ti:Sapphire laser off windows results in a large background. We put two layers of interference filters with a maximum transmission at $\lambda=780$ nm in front of the photodiode to block the scattered light. The photodiode output is integrated for 30 ms while the pulse is passing the probe beam, and again immediately afterward. The difference is taken as the Raman signal. The pulse of atoms arrive at the probe region with a time distribution width (full width at half maximum) of 12 ms, and we use an integration time long enough to include most of them. The sequence of the optical pumping, Raman excitation, and then the detection is shown schematically in Fig. 2.

Before we measure the frequency shift due to the ac Stark effect, we use the Raman transition to probe spin polarization of the LVIS pulse produced by the optical pumping. In Fig. 3 the result of a Raman scan with the optical pumping is

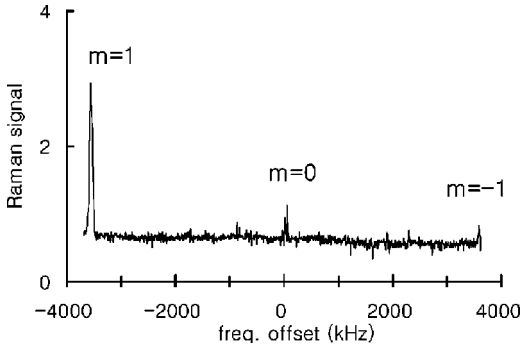

FIG. 3. Spectrum of the stimulated Raman transitions from $|5S_{1/2},F=1,m_F\rangle$ to $|5S_{1/2},F=2,m_F\rangle$ after the optical pumping into the $|5S_{1/2},F=1,m_F=1\rangle$ state. The frequency offset is from the unperturbed hyperfine transition frequency.

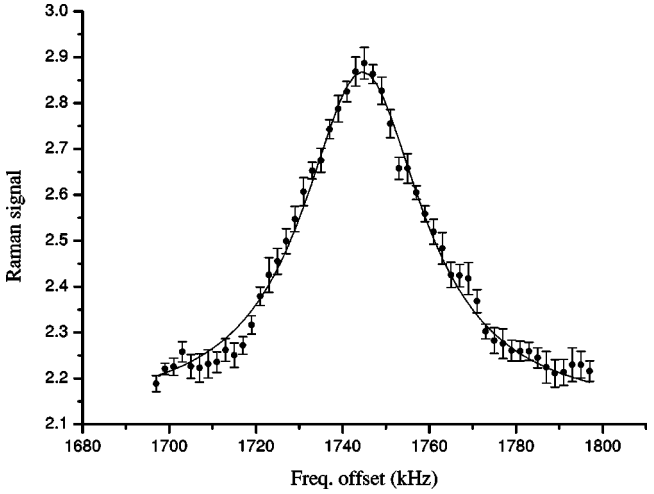

FIG. 4. A typical Raman scan of the transition from the $|5S_{1/2},F=1,m_F=1\rangle$ state to the $|5S_{1/2},F=2,m_F=1\rangle$ state. Black circles are the data points and the solid line is a Lorentzian fit. The full width at half maximum is 33 kHz.

shown. For the scan we use the Raman beam with a 5-mm spot size to cover most of the atoms in the LVIS pulse. Without the Zeeman pumping the $m_F=0$ peak is 2.5 times larger than the $m_F=\pm 1$ peaks, which are of comparable sizes. For the frequency shift measurement, we reduce the Raman beam spot size to 0.73 mm so that it overlaps the tightly focused Stark beam. In Fig. 4 a typical Raman scan for the frequency shift measurement is shown. The scan is made for the transition from $|5S_{1/2},F=1,m_F=1\rangle$ to $|5S_{1/2},F=2,m_F=1\rangle$ on the optically pumped LVIS beam pulse. The Raman laser power in the first-order sidebands is 0.4 mW. The data point at each frequency is obtained by integrating five pulses from the LVIS. The data fits reasonably well to a Lorentzian function with the full width at half maximum of 33 kHz. Roughly 20 kHz is accounted for from the transit-time-limited linewidth, and the remaining part is from the Raman-beam-induced power broadening. When we reduce the Raman beam power the linewidth approaches 20 kHz, but at the expense of the signal size. At the intensities and detunings of the Stark beam used in the measurements (Stark beam wavelength is between 781 and 794 nm), a rubidium atom scatters the Stark beam photon at the rate of 10 Hz or less, and its decoherence effect on the linewidth is negligible.

In order to measure the frequency shift from the vector polarizability we make two consecutive scans like that of Fig. 4 with and without the Stark beam, and compare the center frequencies. We make this measurement at a series of the Stark beam wavelengths from 781 nm to 794 nm. The Stark beam is circularly polarized, and its power is 1.0 W. Qualitatively, the result agrees well with the calculated dependence of β on wavelength (see Fig. 5). In terms of the absolute frequency shift, the measured values show 15% discrepancy with the calculated ones. We ascribe it to the uncertainty in the overlap of the Stark beam and Raman beam. In Fig. 5 we put the overlap factor as a free parameter to obtain the best fit.

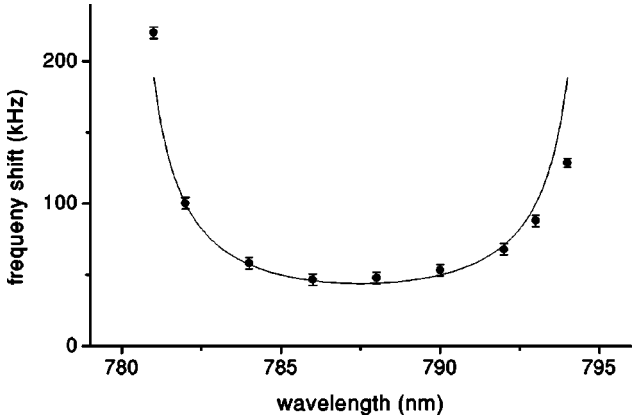

FIG. 5. Measured frequency shift vs the Stark beam wavelength. The solid line is a fit with the theoretical expression $\delta f = \xi\beta(\lambda)|\varepsilon_0|^2$, where the overlap factor ξ is used as the only adjustable fitting parameter.

In another set of measurements, we tune the Stark beam laser to $\lambda=794$ nm, where the frequency shift is sizable, and change its polarization by rotating the quarter-wave plate. The expected frequency shift for the hyperfine transition of interest takes the form

$$\delta f=\beta(\omega)|\varepsilon_0|^2|\hat{\epsilon}\times\hat{\epsilon}^*|, \tag{5}$$

where $\hat{\epsilon}$ is the unit vector representing the Stark beam polarization and $\hat{\epsilon}^*$ is its complex conjugate. We can write Eq. (5) in terms of the angle θ between the linear polarization of the incoming Stark beam and the fast axis of the wave plate as $\delta f=\beta(\omega)|\varepsilon_0|^2\sin 2\theta$. The result of the second set of measurements is shown in Fig. 6. We change the polarization of the Zeeman pumping light to put the atoms in the opposite extreme m_F state $|5S_{1/2},F=1,m_F=-1\rangle$, and find that the frequency shift changes signs accordingly. Finally, when we change the Stark beam intensity we find the frequency shift scales linearly with the intensity. This measurement is made with the circularly polarized light at $\lambda=790$ nm, and the result is shown in Fig. 7.

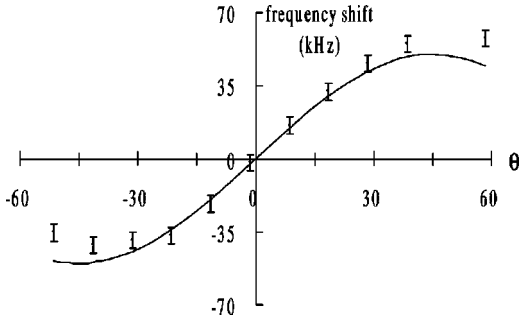

FIG. 6. Measured frequency shift vs the Stark beam polarization. The curve represents the theoretical dependence of $\delta f \propto \sin 2\theta$, where θ is the angle between the linear polarization of the incoming Stark beam and the fast axis of the quarter-wave plate.

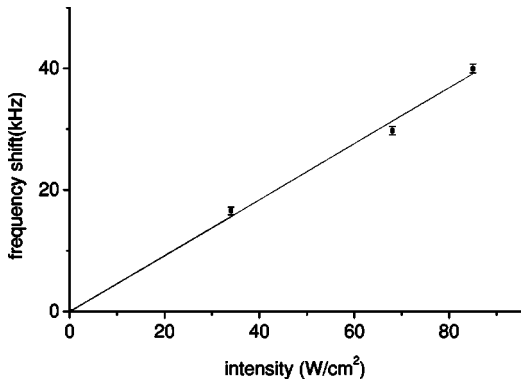

FIG. 7. Measured frequency shift vs the Stark beam intensity.

B. Scalar polarizability

As shown in Eq. (2), the ac Stark shift of the $|5S_{1/2},F,m_F\rangle$ state due to the scalar polarizability is the same for all F and m_F. Consequently, in order to study the scalar part we use the $D2$ transition to the $5P_{3/2}$ state. We use ^{85}Rb for this part of the measurement due to its larger natural abundance. As was pointed out before, for the detunings of interest in this paper the scalar and vector polarizabilities, α and β, of rubidium do not depend on the hyperfine structure or the nuclear spin, and both isotopes of rubidium should produce the same result. We note that the measurement is complicated because the $|5P_{3/2},F,m_F\rangle$ state has its own ac Stark shift, and thus the ac Stark shift in the resonance frequency of the $D2$ transition has contributions from both states. When we use a linearly polarized Stark beam, however, the selection rule $\Delta m_F=0$ implies that the $|5P_{3/2},F'=4,m_F=\pm 4\rangle$ state does not couple with any of the ground states, $|5S_{1/2},F=2\rangle$ and $|5S_{1/2},F=3\rangle$. As a result, neglecting its coupling with the $D_{3/2}$ and $D_{5/2}$ states, the $|5P_{3/2},F'=4,m_F=\pm 4\rangle$ state does not have an ac Stark shift. Explicit expression for the ac Stark shift of the $|5P_{3/2},F,m_F\rangle$ state due to a linearly polarized light can be found from that of the dc Stark effect [14] with proper changes in the energy denominators.

The $D2$ transition has a 6-MHz natural linewidth, and slow atomic beam does not provide any advantage. So we use saturated absorption spectroscopy in a vapor cell for the measurement of the scalar polarizability. The experimental setup is shown in Fig. 8. The quantization axis, z axis, is defined by the B field of 74 Gauss produced by a Helmholtz coil. The probe and saturating beams from a single external-cavity diode laser (probe laser) are of the same circular polarization and counterpropagating along the z axis. The Stark beam to induce the ac Stark shift propagates perpendicular to the z axis, and is linearly polarized along the z axis. The probe beam is split 50/50 before it enters the vapor cell, and only one of the probe beams overlaps the saturating beam. We take the difference between the two probes to eliminate the broad Doppler profile. The profile of the probe beam is cylindrical with characteristic spot sizes of 100 μm and 3 mm along the short and long axes, respectively. The profile of the Stark beam is also cylindrical with spatial dimensions in the probe region of 44 μm and 5.9 mm (the long axis is along the z axis). Elongated probe and Stark beams are used

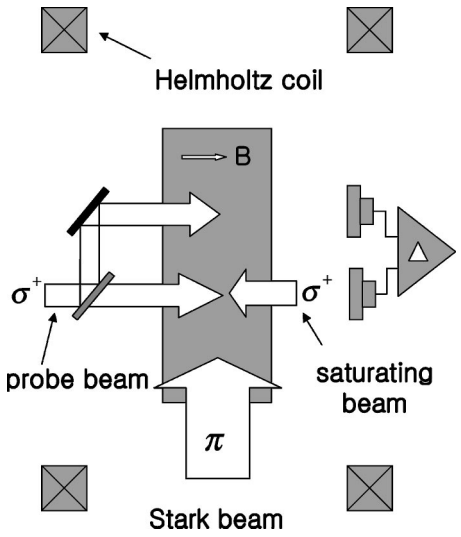

FIG. 8. Saturated absorption setup for the scalar polarizability measurement.

to increase their overlap in the cell. The saturating beam has a four times larger cross-sectional area than the probe beam (roughly 1.3 and 3.0 times long along the long and short axes, respectively) so that it serves as an optical pumping beam, too. The interaction volume defined by the overlapping probe and Stark beams is well embedded in the saturating beam. The resulting spectrum is shown in Fig. 9. The large absorption peak is the resonance signal of the transition, $|5S_{1/2},F=3,m_F=3\rangle$ to $|5P_{3/2},F'=4,m_F=4\rangle$. The resonance is shifted by 104 MHz, consistent with the Zeeman shift at 74 G. The linewidth of 30 MHz is dominated by power broadening from the saturating beam. The probe polarization and the B field direction are arranged so that the frequency of the resonance shifts higher, where there is no interference from other hyperfine or crossover absorption peaks.

In order to use the slope A or B of Fig. 9 for the ac Stark shift measurement, we have another saturated absorption spectrometer for the probe laser that allows us to lock its frequency with a large offset from the unperturbed $|5S_{1/2},F=3\rangle$ to $|5P_{3/2},F'=4\rangle$ transition. The saturating

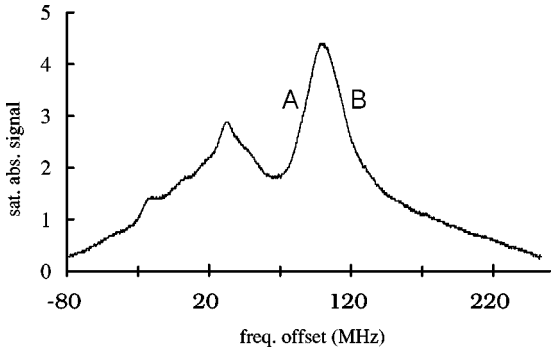

FIG. 9. Saturated absorption spectrum for the scalar polarizability measurement. Frequency offset is from the unperturbed resonance frequency of the cycling transition. Frequency modulation is measured at A and B.

beam for the spectrometer is provided by another external cavity diode laser (auxiliary laser), whose frequency is locked to the low-frequency side slope of the crossover ($F=3$ to $F'=2$ and 3) peak of its own saturated absorption spectrometer. The crossover is 93 MHz red detuned from the $F=3$ to $F'=4$ transition. As a consequence, the saturated absorption spectrum of the probe laser is blueshifted by more than 93 MHz. We lock the probe frequency to the blueshifted peak of the $F=3$ to $F'=4$ transition using the frequency-modulation locking technique. By changing the lock point of the auxiliary laser, we can set the probe frequency near either A or B.

We use the standard phase sensitive detection method for the frequency shift measurement. While the probe-laser frequency is fixed near A using the above locking scheme, the Stark beam power of 1 W for the experimental setup of Fig. 8 is turned on and off by an acousto-optical modulator at the rate of 100 Hz. Change in the $D2$ resonance frequency induced by the Stark beam is also turned on and off, and it leads to a synchronous modulation on the probe absorption. The probe absorption signal is stored and demodulated by a computer to produce a measurement result that is proportional to $\delta s(\mathrm{A})$,

$$\delta s(\mathrm{A}) = \xi \frac{ds}{df}(\mathrm{A})\,\delta f,$$

where $ds/df(\mathrm{A})$ is the slope of the absorption signal at A, ξ is a factor describing the Stark beam and probe beam overlap, and δf is the ac Stark shift. We repeat the measurement at the opposite slope B, and take the difference $\delta s(\mathrm{A}) - \delta s(\mathrm{B})$ as a signature of the ac Stark shift. It allows us to reject the common mode signals from an amplitude modulation or the scattered Stark beam. For the calibration, we measure the slope by modulating the magnetic field by a known amount, and we calculate ξ from the beam geometry.

We carry out this measurement for various wavelengths of the Stark beam between the $D1$ and $D2$ transitions. The experimental results together with the theoretical prediction are shown in Fig. 10. As in the case of the vector polarizability measurement, while the shape, especially the zero crossing, is consistent with theory, there is a discrepancy at the level of 20% for the absolute size of the frequency shifts. We ascribe this to the uncertainty in our estimate of ξ. The experimental curve crosses zero at $\lambda = 790 \pm 0.3$ nm. Calculations show that $\alpha(6S_{1/2})$ is zero at 789.8 nm, and that the frequency shift of the cycling transition vanishes at 790.1 nm. The difference is from the residual shift of the $|5P_{3/2}, F'=4, m_F=4\rangle$ state due to its coupling with the $5D$ states.

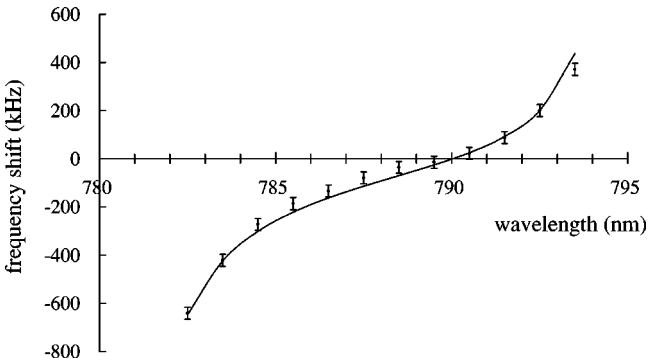

FIG. 10. Frequency shift, or the scalar polarizability of the $5S_{1/2}$ state vs the Stark beam wavelength. The solid line is a theoretical fit that includes all of the couplings, but uses the overlap factor as a free parameter.

IV. CONCLUSION

By independently studying the scalar and vector polarizabilities of rubidium atoms we demonstrate that when the laser is circularly polarized and detuned properly between the $D1$ and $D2$ transitions, the ac Stark shift takes the form of a pure Zeeman shift. This applies to all the alkali atoms, though the magnitude of the effective magnetic field and the photon scatter rate depend on atomic species. The result suggests the possibilities of using a laser beam in place of a static magnetic field and using the laser intensity gradient to produce a Stern-Gerlach force. Since a laser beam can be easily transformed with lenses, made into a standing wave, and used for optical pumping, the Zeeman-like ac Stark shift might find many applications in optical manipulation of atomic motion. For example, in the circularly polarized dipole trap of Ref. [8], the laser light not only provided the potential well but also optically pumped the atoms into the deepest-trappable state.

ACKNOWLEDGMENTS

The authors thank Sang Gu Lee for developing the Raman laser. This work was supported by the Korea Science and Engineering Foundation (Grant No. 971-0204-015-2) and the Ministry of Education (Grant No. 1998-015-D00114).

[1] P. R. Hemmer, M. S. Shahriar, V. D. Natoli, and S. Ezekiel, J. Opt. Soc. Am. B **6**, 1519 (1989).
[2] R. Grimm, M. Weidenmüller, and Yu. B. Ovchinnikov, Adv. At., Mol., Opt. Phys. **42**, 95 (2000).
[3] C. S. Adams, M. Sigel, and J. Mlynek, Phys. Rep. **240**, 143 (1994).
[4] C. Cohen-Tannoudji and J. Dupont-Roc, Phys. Rev. A **5**, 968 (1972).
[5] M. Rosatzin, D. Suter, and J. Mlynek, Phys. Rev. A **42**, 1839 (1990).
[6] M. Zielonkowski, J. Steiger, U. Schunemann, M. DeKieviet, and R. Grimm, Phys. Rev. A **58**, 3993 (1998).
[7] D. Cho, J. Korean Phys. Soc. **30**, 373 (1997).
[8] K. L. Corwin, S. J. M. Kuppens, D. Cho, and C. E. Wieman, Phys. Rev. Lett. **83**, 1311 (1999).
[9] In the study of dc Stark effect, it is conventional to express the

shift as $-\alpha_0|\mathbf{E}|^2/2$. See, for example, A. Khadjavi, A. Lurio, and W. Happer, Phys. Rev. **167**, 128 (1968). The expression in Eq. (1) reduces to that of the dc Stark shift with the identification of $\alpha_0=-\alpha(0)$ and with the replacement of $\mathcal{E}_0\cdot\mathcal{E}_0^*$ with the mean squared value of $\mathbf{E}(t)$.

[10] J. D. Miller, R. A. Cline, and D. Heinzen, Phys. Rev. A **47**, R4567 (1993).

[11] N. F. Ramsey, *Molecular Beams* (Oxford University Press, London, 1956).

[12] Z. T. Lu, K. L. Corwin, M. J. Renn, M. H. Anderson, E. A. Cornell, and C. E. Wieman, Phys. Rev. Lett. **77**, 3331 (1996).

[13] M. S. Jun, C. Y. Park, and D. Cho, J. Korean Phys. Soc. **33**, 260 (1998).

[14] H. L. Zhou and D. W. Norcross, Phys. Rev. A **40**, 5048 (1989).